U. of Iowa 66-48

N67 12262
(ACCESSION NUMBER)

55
(PAGES)

CR-80113
(NASA CR OR TMX OR AD NUMBER)

(THRU)
/

(CODE)
39

(CATEGORY)

FACILITY FORM 602

GPO PRICE $ _____

CFSTI PRICE(S) $ _____

Hard Copy (HC) __3.00__

Microfiche (MF) __.50__

653 July 65

Department of Physics and Astronomy
THE UNIVERSITY OF IOWA

Iowa City, Iowa

SEVERAL OBSERVATIONS OF LOW-ENERGY
PROTONS AND ELECTRONS IN THE
EARTH'S MAGNETOSPHERE
WITH OGO 3*

by

L. A. Frank

Department of Physics and Astronomy
University of Iowa
Iowa City, Iowa

November 1966

Abstract

/ 2262

Simultaneous observations of proton (190 eV $\leq$ E $\leq$ 48 keV) and electron (170 eV $\leq$ E $\leq$ 46 keV) differential energy spectrums during segments of three outbound traversals of OGO 3 through the magnetosphere for the period 11-15 June 1966 on L-shells 3.3 to 16 are presented. Proton intensities at L = 4 on 15 June 1966 were 8 x 10^5 $(cm^2\text{-sec-sr})^{-1}$ (330 $\leq$ E $\leq$ 530 eV), $\lesssim$ 1.5 x 10^6 $(cm^2\text{-sec-sr})^{-1}$ (4.7 $\leq$ E $\leq$ 7.6 keV) and $\lesssim$ 10^6 $(cm^2\text{-sec-sr})^{-1}$ (16 $\leq$ E $\leq$ 26 keV) and at L = 7.5 were $\leq$ 5 x 10^4 $(cm^2\text{-sec-sr})^{-1}$ (330 $\leq$ E $\leq$ 530 eV), 4 x 10^6 $(cm^2\text{-sec-sr})^{-1}$ (4.7 $\leq$ E $\leq$ 7.6 keV) and 6 x 10^6 $(cm^2\text{-sec-sr})^{-1}$ (16 $\leq$ E $\leq$ 26 keV) with local pitch angles 78° ($\pm$ 4°) and at a geomagnetic latitude 23° ($\pm$ 1°). Peak intensities of protons (30 $\leq$ E $\leq$ 48 keV) were observed at L $\sim$ 7.0. A preliminary order-of-magnitude estimate of the total energy of trapped protons/(190 eV $\leq$ E $\leq$ 48 keV) within the earth's magnetosphere is 5 x 10^{21} ergs and the estimated contribution from this low-energy proton distribution to the quiet-time terrestrial ring current field at the earth's surface is $\sim$ -10 γ. A transient, narrow peak of relatively high low-energy proton and electron

Author

intensities within the energy range $\sim$ 300 eV to 2 keV at L $\sim$ 4

with width $\Delta L \sim 1$ is also observed. Typical characteristics

of proton and electron intensity 'spikes' at peak intensities

in the late evening sector of the earth's magnetic tail are

(a) approximately equal proton (190 eV $\leq$ E $\leq$ 48 keV) and

electron (170 eV $\leq$ E $\leq$ 46 keV) energy densities, $\sim 10^{-9}$

erg(cm)$^{-3}$ each, (b) approximately equal proton and electron

densities over the above energy range, ~ 1 (cm)$^{-3}$ each, and

(c) largely dissimilar differential energy spectrums, proton

spectrums with intensity peaks noncoincident in energy with

those of the electron intensity peaks and significantly broader

(harder) in the high-energy tail (E $\gtrsim$ 3 keV) than the relatively

steep (soft) electron spectrums in this energy range.

I. Introduction

Observations of low-energy protons and electrons over the energy range extending from approximately 100 eV to 100 keV within the earth's magnetosphere are essential toward the understanding of many magnetospheric phenomena including the terrestrial ring currents, the acceleration processes responsible for the corpuscular radiation precipitated into the auroral regions, the plasmas within the earth's magnetic tail, and the sources of higher energy protons and electrons populating the earth's radiation zones. This initial survey of low-energy electrons and protons over geocentric radial distances ranging from 3 R_E to 15 R_E (R_E, earth radius) with measurements obtained with a sensitive electrostatic analyzer device borne on the earth-satellite OGO 3 is intended to provide an introduction to several of the characteristics of the spatial distributions of electrons and protons over an energy range 200 eV to 50 keV within the earth's magnetosphere near the magnetic equatorial plane. The search for the terrestrial ring currents by in situ measurements is continued in the present investigation [cf Davis, 1965; Hoffman and Bracken, 1965; Cahill, 1966; Frank, 1966a] during a

period of relative magnetic quiescence, and several features
of the charged particle distributions at the boundary of
durable trapping of charged particles by the geomagnetic field
at geocentric radial distances approximately 8 R_E in the
evening sector of the earth's magnetosphere are clarified.
Simultaneous observations of the differential energy spectrums
of electrons and protons, separately, over the aforementioned
energy range are presented herein for regions in the earth's
magnetic tail and deep within the radiation zones and will be
important in delineating prominent acceleration mechanisms
providing 'local' acceleration of charged particles within the
earth's magnetosphere and its environs. The spirit of the
following discussion is directed toward an exploratory examination
of low-energy proton and electron intensities in the earth's
magnetosphere with unique and discriminative observations.

II. Description of Apparatus

OGO 3 (1966-49A) was launched at 02:48 U.T. on 7 June
1966 into a highly eccentric orbit with initial apogee 128,500 km
and perigee 6,700 km geocentric radial distances, inclination
31° and period 48.6 hours. At launch the local time of the
direction from the center of earth to spacecraft apogee position
was ~ 22:00. A composite system of reaction wheels and gas
jets provided a predetermined, monitored orientation of the
various spacecraft coordinates with respect to the directions
from the satellite to earth and the sun and with respect to
the orbital plane. The University of Iowa instrumentation
includes four cylindrical-plate electrostatic analyzers to
select charged particle energy and continuous channel multipliers
(Bendix 'channeltrons') as charged particle detectors. Each of
the two pairs of electrostatic analyzers provides simultaneous
measurements of the intensities of protons and electrons,
separately, within the same energy bandpasses over an energy
range extending from approximately 100 eV to 50,000 eV. The
directions of the fields of view of these two pairs of electro-
static analyzers, designated as LEPEDEA's 'A' and 'B', are

orthogonal and are directed parallel to spacecraft body Cartesian

axes, + Z (toward earth during normal spacecraft operations) and

+ Y, respectively. Two EON type 213 Geiger-Mueller tubes

(1.2 mg(cm)$^{-2}$ mica windows) were positioned in the instrument

package such that the directions of their collimated fields of

view were parallel to those of the electrostatic analyzer pairs.

More detailed descriptions of the instrumentation have been

given previously by Frank [1966b]. The energy bandpasses for

the proton and electron channels of LEPEDEA 'B' are summarized

in Table I (protons) and Table II (electrons). Observations

with the second pair of electrostatic analyzers, LEPEDEA 'A',

will be reported in a forthcoming survey of the angular

distributions of low-energy protons and electrons.

TABLE I

OGO 3 LEPEDEA PROTON CHANNELS 'B'

ENERGY BANDPASSES

Proton Channel	Energy Bandpass*
3pB	90 - 150 eV
4pB	190 - 320 eV
5pB	330 - 530 eV
6pB	450 - 720 eV
7pB	690 - 1100 eV
8pB	1.1 - 1.8 keV
9pB	1.8 - 2.9 keV
10pB	3.3 - 5.3 keV
11pB	4.7 - 7.6 keV
12pB	6.7 - 11 keV
13pB	11 - 18 keV
14pB	16 - 26 keV
15pB	30 - 48 keV

*Analyzer constant is 7.6 eV $(volt)^{-1}$

TABLE II

OGO 3 LEPEDEA ELECTRON CHANNELS 'B'

ENERGY BANDPASSES*

Electron Channel	Energy Bandpass**
3eB	80 - 140 eV
4eB	170 - 300 eV
5eB	280 - 500 eV
6eB	380 - 680 eV
7eB	610 - 1100 eV
8eB	940 - 1700 eV
9eB	1.5 - 2.7 keV
10eB	2.8 - 5.0 keV
11eB	4.1 - 7.2 keV
12eB	5.8 - 10 keV
13eB	9.8 - 17 keV
14eB	14 - 24 keV
15eB	26 - 46 keV

*See also Frank [1966b]

**Analyzer constant is 7.3 eV (volt)$^{-1}$

III. Observations

An example of the LEPEDEA 'B' responses to low-energy proton and electron intensities in the earth's magnetosphere is provided in Figure 1 which displays the counting rate profiles of channels 12eB (electrons, $5.8 \leq E \leq 10$ keV) and 15pB (protons, $30 \leq E \leq 48$ keV) and of the 213B G.M. tube as functions of magnetic shell parameter L for the outbound pass of OGO 3 on 13 June 1966. Several useful position coordinates for these observations, geomagnetic latitude (λ_m), solar magnetospheric latitude (θ_{SM}) [Ness, 1965], and solar ecliptic latitude and longitude (θ_{SE}, φ_{SE}) are shown in Figure 2. The motion of the spacecraft during this period was characterized by a trace from L = 6.5 to 16 through the late evening sector of the earth's magnetosphere at moderate solar ecliptic and solar magnetospheric latitudes (θ_{SE}, $\theta_{SM} \sim 35°$); the axes of the fields of view of the LEPEDEA 'B' electrostatic analyzers and of the 213B G. M. tube were directed within $\lesssim 30°$ of the anti-solar direction throughout the period of observations shown in Figure 1 (see Appendix, Table V). Although no comparison of these observations with simultaneous measurements of the magnetic fields is provided

here, all observations were obtained at geocentric radial

distances $\lesssim$ 16 R_E in the late evening sector of the magnetosphere

and can be positioned interior to the magnetopause with good

certainty by comparison of the OGO 3 trajectory during this

period with IMP 1 observations of the position of the magneto-

pause [Ness, Scearce and Seek, 1964].

Salient features of the observations presented in Figure

1 include (a) a decrease in proton ($30 \leq E \leq 48$ keV) intensities

coincident with a decrease in electron ($E > 45$ keV) intensities

at L $\sim$ 7.5 to 8.0, (b) an increase in electron ($5.8 \leq E \leq 10$ keV)

intensities by a factor $\sim$ 40 coincident with the decrease in

electron ($E > 45$ keV) and proton ($30 \leq E \leq 48$ keV) intensities

at L $\sim$ 7.5 to 8.0 and (c) the occurrence of intensity 'spikes'

beyond L $\sim$ 9 in each of the three intensity profiles. These

sporadic increases in proton ($30 \leq E \leq 48$ keV) and electron

($5.8 \leq E \leq 10$ keV and $E > 45$ keV) intensities beyond L $\sim$ 9 are

coincident within the resolution of the abridged set of observations

summarized in Figure 1. (For example, approximately 3×10^3

individual telemetered samples of the responses of each of

these three channels, and of each of the remaining 63 channels

not displayed in Figure 1, are available during the period of

this single segment of data.) Although several increases of

proton ($30 \leq E \leq 48$ keV) and electron ($5.8 \leq E \leq 10$ keV)

intensities occur without a measurable increase in electron

($E > 45$ keV) intensities reflected in the responses of the

213B G.M. tube at $L \gtrsim 13$, such an observation may be a mani-

festation of the generally decreasing character of the intensities

as a function of L to intensity levels below the threshold of

the G.M. tube, $\sim 2 \times 10^3$ $(cm^2-sec-sr)^{-1}$. The electron

($5.8 \leq E \leq 10$ keV) and proton ($30 \leq E \leq 48$ keV) intensities

are, in an average sense, decreasing with increasing L-value

beyond $L \sim 8.0$; these decreases in intensities from $L \sim 8.0$ to

15 are by factors ~ 200 and ~ 10, respectively, for the outbound

pass on 13 June 1966. The relatively high electron ($5.8 \leq E \leq 10$ keV)

channel counting rates over $L \sim 7.5$ to 13.5 shown in Figure 1 are

characteristic of the responses of the present instrumentation in the

region of large low-energy electron intensities in the dark hemisphere

of the magnetosphere beyond $L \sim 8$ reported by Gringauz and co-workers

[1960, 1963] and by Freeman [1964] (see Frank [1966b] for detailed

measurements of electron differential energy spectrums, energy

densities, omnidirectional integral intensities, etc.). For the

'spike' of intensities at $L \sim 13.2$, typical electron

(170 eV $\leq E \leq 46$ keV) energy densities and number densities are

3 ($\pm$ 1) x 10^{-9} erg(cm)$^{-3}$ and 0.7 ($\pm$ 2) electrons (cm)$^{-3}$ and

typical proton (190 eV $\leq$ E $\leq$ 48 keV) energy densities and

number densities are 4 ($\pm$ 2) x 10^{-9} erg(cm)$^{-3}$ and 0.6 ($\pm$ 2)

protons (cm)$^{-3}$, respectively. These values are judged to be

accurate within a factor of 2 (see Frank [1966b] for discussion

of calculations of these omnidirectional quantities). The

equalities of proton and electron energy densities and number

densities within the above energy ranges and experimental error

are characteristic of the present observations of the intensity

'spikes' observed in the midnight and evening sectors of the

magnetosphere but exceptions to this situation have already

been found and will be discussed in a later, more thorough

analysis.

The rapid decrease of electron (E > 45 keV) intensities

at L $\sim$ 7.5 to 8.0 bracketed at lower L-values by a relatively

smooth, high intensity profile and at higher L-values by a

fluctuating, lower intensity profile as exemplified in Figure 1

has been interpreted as delineating the outermost boundary of

the durable trapping of charged particles in the magnetosphere

[cf Frank, 1966c; Anderson, 1965]. This interpretation is

further supported by the similar behavior of the profile of

proton ($30 \leq E \leq 48$ keV) intensities and the discontinuity
in the electron ($5.8 \leq E \leq 10$ keV) intensity profile at
$L \sim 7.5$.

Another example of low-energy proton and electron
intensities as functions of magnetic shell parameter
L is shown in Figure 3 for $L \sim 3.3$ to 14.5 during the outbound
pass on 15 June 1966. Several useful coordinates for this
segment of data are displayed in Figure 4 and directions of
the axes of the fields of view are summarized in the Appendix.
The profiles of proton ($450 \leq E \leq 720$ eV and $16 \leq E \leq 26$ keV)
and electron ($1.5 \leq E \leq 2.7$ keV) intensities shown in Figure 3
reveal several interesting features of the distributions of low-
energy charged particles within the magnetosphere, (a) a narrow
region of proton ($450 \leq E \leq 720$ eV) intensities centered at
$L = 4$ with width $\Delta L \sim 1$, (b) significant proton ($16 \leq E \leq$
26 keV) intensities above background responses of the instru-
mentation in a region extending from $L \sim 5.0$ to 9.0, (c) a
third locale at $L \sim 9$ to 12 with relatively low proton
($450 \leq E \leq 720$ eV and $16 \leq E \leq 26$ keV) intensities but with
enhanced electron ($1.5 \leq E \leq 2.7$ keV) intensities, (d) a second
narrow maximum of proton ($450 \leq E \leq 720$ eV) intensities centered
at $L \sim 12.7$ with width $\Delta L \sim 1$, and (e) relatively constant

intensities of electrons ($1.5 \leq E \leq 2.7$ keV) from $L \sim 3.5$ to 9.

Unidirectional proton intensities in eight energy bandpasses in the

energy range extending from 330 eV to 48 keV as functions of

L are presented in Figures 5, 6 and 7. It is easily noted that

(a) the narrow proton maximum at $L \sim 4$ is predominantly

populated by protons with energies $\lesssim 2$ keV, (b) proton

($E \gtrsim 5$ keV) intensities are concentrated in a region extending

from $L \sim 5$ to 10, (c) fine structure exists in the profiles

of proton ($E \lesssim 26$ keV) intensities beyond $L \sim 8$, attributable

to temporal and/or spatial variations in intensities, and

(d) there is a maximum in proton ($30 \leq E \leq 48$ keV) intensities

at $L \sim 7$, 4.5×10^6 $(cm^2\text{-sec-sr})^{-1}$. Proton intensities at

$L = 4$ are 8×10^5 $(cm^2\text{-sec-sr})^{-1}$ ($330 \leq E \leq 530$ eV), $\lesssim 1.5 \times 10^6$

$(cm^2\text{-sec-sr})^{-1}$ ($4.7 \leq E \leq 7.6$ keV) and $\lesssim 10^6$ $(cm^2\text{-sec-sr})^{-1}$

($16 \leq E \leq 26$ keV); at $L = 7.5$ proton intensities are $\leq 5 \times 10^4$

$(cm^2\text{-sec-sr})^{-1}$ ($330 \leq E \leq 530$ eV), 4×10^6 $(cm^2\text{-sec-sr})^{-1}$

($4.7 \leq E \leq 7.6$ keV) and 6×10^6 $(cm^2\text{-sec-sr})^{-1}$ ($16 \leq E \leq 26$ keV).

These unidirectional intensities were obtained at geomagnetic

latitude $\lambda_m = 22°$ (Figure 4) with local pitch angle $\alpha = 81°$

(see Appendix) at $L = 4.0$, and $\lambda_m = 24°$ with $\alpha = 74°$ at $L = 7.5$.

A further segment of observations of low-energy proton

intensities within the magnetosphere is summarized in Figure 8

which displays the proton intensities in six discrete energy

bandpasses within the energy range 190 eV to 26 keV as

functions of L during the outbound pass on 11 June 1966 (refer

to Figure 9 and Appendix for several useful coordinates).

The transition of the character of these profiles with decreasing

bandpass energy from higher proton ($5.3 \leq E \leq 26$ keV) intensities

at $L \lesssim 10$ to higher proton ($190 \leq E \leq 720$ eV) intensities at

$L \gtrsim 10$ over the L-value range, 7 to 13, is easily discernible.

Proton unidirectional intensities observed during this out-

bound pass are similar in magnitudes to proton intensities

measured at these L values during the outbound pass on 15 June

(cf Figures 5, 6 and 7) although details in the structure of the

intensity profiles are dissimilar.

Simultaneous observations of the low-energy proton and

electron differential energy spectrums near the low-energy

proton maximum observed at $L \sim 4$ during the outbound pass on

15 June (see Figure 5) are shown in Figure 10. These electron

and proton spectrums monotonically increase with decreasing

particle energy with significant response above background

rates of the instrumentation to proton and electron intensities

over the energy range extending from 190 eV to 1.8 keV and
280 eV to 46 keV, respectively. The monotonic decline of
the electron and proton spectrums with increasing energy over
the energy range extending from $\sim$ 300 eV to 2 keV and the constant
ratio of the number density of protons and electrons per unit
energy interval, $(dN_e/dE)/(dN_p/dE)^{-1} = 1.6$ ($\pm$ 0.7) where
(dN_e/dE) is the differential number density of electrons, over
the above energy range suggest that these low-energy proton
and electron intensities are the signature of the high-energy
tail of a thermalized plasma with peak differential intensities,
$\frac{dJ}{dE}$, at $E \lesssim 200$ eV. The energy densities and number densities
of electrons (170 eV $\leq E \leq$ 2.7 keV) and protons (190 eV $\leq E \leq$
2.9 keV) are each 4 ($\pm$ 2) x 10^{-9} erg(cm)$^{-3}$ and 6 ($\pm$ 2) (cm)$^{-3}$,
respectively. These low-energy proton and electron intensities
at $L \sim 4$ are a transient and variable feature of the distri-
bution of charged particles in this region and will be discussed
in a forthcoming investigation.

The results of a preliminary comparison of the present
observations of the proton differential energy spectrum over
the energy range extending from 1.8 keV to 48 keV on 15 June
1966 and Explorer 14 measurements of the proton ($E \geq$ 97 keV)

spectrum at L = 6.0 in late 1962 are summarized in Figure 11.
The proton differential energy spectrum labelled with Explorer
14 has been calculated from the integral energy spectrum at
L = 6.0, E.P.A. = 65° (E.P.A., equatorial pitch angle) reported
by Davis [1965]; the OGO 3 observations shown in Figure 11 are
also for L = 6.0 but with E.P.A. = 45°. This disparity in
values of E.P.A. will be reflected in the proton (E ~ 100 keV)
intensities by factors $\lesssim$ 2 [Davis, 1965]. Although the two
observations of proton spectrums do not overlap in energy and
are separated by a period of almost three years, no disturbing
disagreement is judged to be evident in the initial comparison
of spectrums displayed in Figure 11.

Two exemplary measurements of the low-energy proton and
electron differential energy spectrums are shown in Figures 12
and 13 at positions in the late evening sector of the magnetosphere
at 10.5 R_E on 15 June and at 15.9 R_E on 14 June 1966, respectively.
Salient features of these spectrums include (a) a proton spectrum
which is significantly broader than the simultaneously measured
electron spectrum and (b) noncoincidence of the differential
intensity peaks in proton and electron spectrums (for example,
the proton and electron intensity peaks are at ~ 1.5 keV and

~ 700 eV, respectively, for the observations shown in Figure 12). Further, it is noted that the peak proton intensities are not consistently occurring at higher energies than the peak in electron intensities (see Figure 12) but also may occur at lower energies (see Figure 13). For the electron and proton energy spectrums displayed in Figure 12, the energy densities and number densities of protons (190 eV $\leq$ E $\leq$ 48 keV) and electrons (170 eV $\leq$ E $\leq$ 46 keV) are each 4 ($\pm$ 2) x 10^{-9} erg(cm)$^{-3}$ and 1 ($\pm$ 0.5) (cm)$^{-3}$, respectively.

IV. <u>Discussion</u>

Several initial observations of low-energy proton and electron intensities within the evening sector of the earth's magnetosphere have been presented in the preceding discussion. Many features of the spatial distributions of these low-energy charged particles within the energy range extending from ~ 200 eV to 50 keV are self-evident upon perusal of the Figures. Each of the topics which have been cursorily examined here will be dealt with in future investigations with considerably more detail. However, several characteristics of these spatial distributions of low-energy proton and electron intensities are worthy of further discussion.

It is of interest to compare the energy density of protons (190 eV $\leq$ E $\leq$ 48 keV) observed during the outbound pass of OGO 3 through the outer radiation zone on 15 June 1966 with the largest reservoir of charged particle energy within the magnetosphere which has been observed by direct detection to the present date (protons, E $\geq$ 97 keV [Davis, 1965]). These observations of proton (190 eV $\leq$ E $\leq$ 48 keV) energy densities at λ_m = 22°($\pm$ 2°), the corresponding magnetic field energy density $B^2/8\pi$, and

Explorer 14 measurements of proton ($E \geq 97$ keV) energy densities
at the geomagnetic equator during late 1962 are summarized for
several values of L in Table III. No geomagnetic storms were
reported during the period of the present OGO 3 observations
[High Altitude Observatory Preliminary Report of Solar Activity,
TR 773] and these low-energy proton intensities are presumably
representative of the quiet-time proton distributions in the
outer radiation zone. Although the geomagnetic latitudes and
epochs of these two observations significantly differ it is
clearly instructive to compare the energy densities of these two
proton distributions. The ratios of proton (190 eV $\leq E \leq 48$ keV)
energy densities to proton ($E \geq 97$ keV) energy densities are
$\sim 4 \times 10^{-3}$ at L = 3.6 (near peak of proton ($E \geq 97$ keV) energy
density), ~ 1 at L = 5.7, and ~ 4 at L = 6.5. Hence at L $\sim$ 3.5
protons within the energy range 190 eV to 48 keV provide an
insignificant contribution to the quiet-time terrestrial ring
current relative to that of the proton ($E \geq 97$ keV) populations,
but for L $\gtrsim$ 5 the proton (190 eV $\leq E \leq 48$ keV) contribution to
the ring current on a given L-shell is similar or greater than
that attributable to proton ($E \geq 97$ keV) intensities. Since the
relative contribution of these two proton populations to the

TABLE III

Comparison of OGO 3 Measurements of
Proton (190 eV $\leq$ E $\leq$ 48 keV) Energy Densities (15 June, 1966)
with Explorer 14 Observations of Proton (E $\geq$ 97 keV) Energy Densities (1962)*

L	OGO 3 Proton (190 eV $\leq$ E $\leq$ 48 keV) Energy Density, erg(cm)$^{-3}$ λ_m = 22° ($\pm$ 2°)	$\frac{B^2}{8\pi}$, erg(cm)$^{-3}$** λ_m = 22° ($\pm$ 2°)	EXPLORER 14* Proton (E $\geq$ 97 keV) Energy Density, erg(cm)$^{-3}$ λ_m = 0°
3.6	1.4×10^{-9}	5.5×10^{-6}	3.2×10^{-7}
4.7	5.0×10^{-9}	1.4×10^{-6}	1.1×10^{-7}
5.2	2.1×10^{-8}	8.4×10^{-7}	5.6×10^{-8}
5.7	2.8×10^{-8}	5.2×10^{-7}	3.2×10^{-8}
6.5	3.9×10^{-8}	2.3×10^{-7}	9.6×10^{-9}
7.5	3.4×10^{-8}	1.0×10^{-7}	- - -
8.2	4.1×10^{-8}	5.7×10^{-8}	- - -
9.5	1.3×10^{-8}	2.0×10^{-8}	- - -
10.0	7.1×10^{-9}	1.3×10^{-8}	- - -

*Davis [1965]

**Jensen and Cain [1962]

quiet-time terrestrial ring current is approximately proportional

to the ratio of their total kinetic energies [cf Parker, 1966], it

is also instructive to estimate the magnitude of the reservoir of

kinetic energy of the proton (190 eV $\leq$ E $\leq$ 48 keV) distribution.

The total kinetic energy of protons (E $\geq$ 97 keV) within the earth's

magnetosphere has been shown to be $\sim$ 6 $\times$ 10^{21} ergs [Hoffman and

Bracken, 1965]; an order-of-magnitude estimate of the total proton

(190 eV $\leq$ E $\leq$ 48 keV) kinetic energy for the observations reported

here, assuming azimuthal symmetry over L = 5 to 10 and a dependence

of the observed energy densities (Table III) upon geomagnetic

latitude λ_m by factors $\lesssim$ 3 over λ_m = 0° to 30°, is $\sim$ 5 $\times$ 10^{21} ergs,

or approximately the same magnitude as the trapped proton

(E $\geq$ 97 keV) energy reservoir. Hence it is quite likely that the

proton (190 eV $\leq$ E $\leq$ 48 keV) contribution to the quiet-time

proton ring current is similar to that due to the outer zone

protons (E $\geq$ 97 keV), $\sim$ -10 γ (1 γ = 10^{-5} gauss) at the surface

of the earth [cf Hoffman and Bracken, 1965]. Further inspection

of Table III and comparison of the OGO 3 measurements of proton

(190 eV $\leq$ E $\leq$ 48 keV) energy densities with the magnetic field

energy density, where B has been calculated at the satellite

position with the Jensen and Cain [1962] coefficients derived

from survey data at the earth's surface, show that the proton

(190 eV $\leq$ E $\leq$ 48 keV) energy densities should contribute

substantially to the distortion of the geomagnetic field for

$6 \lesssim L \lesssim 10$. Comparison of simultaneous OGO 3 measurements of the

vector magnetic field with the above observations of charged

particle intensities is vital in determining the detailed effect

of this low-energy proton distribution upon the local magnetic

fields.

A narrow peak of relatively high low-energy proton and

electron intensities within the energy range $\sim$ 300 eV to 2 keV

at L $\sim$ 4 with width $\Delta L \sim$ 1 has been observed during several

OGO 3 traversals of the outer radiation zone (see Figures 3 and

5). The absence of the intensity peak at these L-values during

many of the segments of data through this region which have

been perused to date indicates that measurable intensities of

these low-energy protons and electrons are a transient phenomena.

The proton and electron differential energy spectrums share a

common slope and an almost equal number density per unit energy

interval and monotonically increase with decreasing energy over

the energy range extending from $\sim$ 300 eV to 2 keV, which suggest

that these spectrums may be the signatures of the high energy

tail of a thermalized plasma with peak differential intensities

at $E \lesssim 200$ eV. The energy densities and number densities of

electrons (170 eV $\leq$ E $\leq$ 2.7 keV) and protons (190 eV $\leq$ E $\leq$ 2.9 keV)

are equal, $4(\pm 2) \times 10^{-9}$ erg(cm)$^{-3}$ and $6(\pm 2)$ cm^{-3}, respectively,

at the peak intensities on L $\sim$ 4. The total inventory of charged

particle kinetic energy over the above energy range in this region

is inadequate to contribute significantly to a quiet-time

terrestrial ring current.

All observations of low-energy protons presented here are

in agreement with the upper limits on proton intensities in this

energy range obtained with an electrostatic analyzer borne on

IMP-1 as reported by Wolfe, Silva and Myers [1966]. These low-

energy proton intensities observed with OGO 3 are near or below

the intensity threshold of the IMP 1 instrument. The threshold

omnidirectional intensity for the IMP 1 apparatus is 7.2×10^{4}

(cm^2-sec-ev)$^{-1}$ at 600 eV [Wolfe, et al, 1966]; the threshold

omnidirectional intensity for the OGO 3 LEPEDEA 'B' instrument is

2.5×10^2 (cm^2-sec-ev)$^{-1}$ at 585 eV.

First simultaneous observations of proton and electron

differential energy spectrums over the energy range extending

from ~ 200 eV to 50 keV in the late evening sector of the

earth's magnetic tail are displayed in Figures 12 and 13.

Observations of intensity 'spikes' of electrons (E > 45 keV)

associated with the high-energy tails of the electron spectrums

have been reported by Frank [1965], Anderson [1965] and

Anderson and Ness [1966]. Several observations of the electron

($350 \leq E \leq 20$ keV) spectrums at ~ 17 R_E with the Vela satellites

have been summarized by Coon [1966], and measurements over the

energy range extending from ~ 100 eV to 50 keV in the earth's

magnetic tail at geocentric radial distances 8 R_E to 20 R_E

have been recently reported by Frank [1966b]. Typical character-

istics of these intensity 'spikes' at peak intensities

(refer to Figure 13 for exemplary proton and electron

differential energy spectrums) are (a) approximately equal

proton (190 eV $\leq E \leq 48$ keV) and electron (170 eV $\leq E \leq 46$ keV)

energy densities, ~ 10^{-9} erg$(cm)^{-3}$ each, (b) approximately equal

proton and electron number densities over the above energy range,

~ 1 $(cm)^{-3}$ each, and (c) largely dissimilar differential energy

spectrums, proton spectrums with intensity peaks noncoincident

with those of the electron intensity peaks and significantly

broader (harder) in the high energy tail (E $\gtrsim$ 3 keV) than the

relatively steep (soft) electron spectrums. Typical omnidirectional
intensities of protons ($E \geq 190$ eV) and electrons ($E \geq 170$ eV)
in the maxima of these intensity 'spikes' beyond ~ 10 R_E are
$\sim 5 \times 10^7$ $(cm^2\text{-sec})^{-1}$ and $\sim 10^9$ $(cm^2\text{-sec})^{-1}$, respectively.

Finally, it is noted here that the peaks of proton
($30 \leq E \leq 48$ keV, $16 \leq E \leq 26$ keV, and $11 \leq E \leq 18$ keV)
intensities occur, in a coarse manner, on lower L-shells with
increasing proton energy (see Figure 7), which may be
characteristic of radial diffusion of protons within this energy
range [cf Nakada, Dungey and Hess, 1965]. For proton energies
$E \lesssim 11$ keV (see Figures 5 and 6) this increase of the L-shell
coordinate of the 'average' peak of intensities with decreasing
proton energy is not clearly evident. Further mapping of these
low-energy proton intensities and a comprehensive survey of
the temporal variations in intensities are now in progress.

Appendix

The following Tables summarize the directions of the axis of the LEPEDEA 'B' field of view in several useful coordinate systems for the three consecutive outbound passes of OGO 3 through the earth's magnetosphere presented in the preceding discussions.

TABLE IV

11 JUNE 1966 (OUTBOUND)

Satellite Position, L	Axis directed along:				Pitch angle*, α**
	Solar-ecliptic		Solar-magnetospheric		
	θ_{SE}	φ_{SE}	θ_{SM}	φ_{SM}	
8	-4°	186°	-4°	186°	76°
10	-8°	191°	-7°	192°	71°
12	-12°	195°	-10°	196°	65°

TABLE V

13 JUNE 1966 (OUTBOUND)

Satellite Position, L	Axis directed along:				
	Solar-ecliptic		Solar-magnetospheric		Pitch angle*,
	θ_{SE}	φ_{SE}	θ_{SM}	φ_{SM}	α**
7	-1°	182°	-1°	182°	77°
8	-3°	185°	-3°	185°	75°
10	-8°	190°	-7°	191°	70°
12	-12°	194°	-10°	195°	63°
14	-16°	197°	-13°	198°	55°
16	-19°	198°	-18°	199°	48°

TABLE VI

15 JUNE 1966 (OUTBOUND)

Satellite Position, L	Axis directed along:				Pitch angle*, α**
	Solar-ecliptic		Solar-magnetospheric		
	θ_{SE}	φ_{SE}	θ_{SM}	φ_{SM}	
4	5°	168°	5°	168°	81°
5	3°	174°	3°	174°	79°
6	1°	178°	1°	178°	77°
8	-3°	185°	-3°	185°	73°
10	-7°	189°	-6°	191°	68°
12	-11°	193°	-9°	194°	62°
14	-15°	196°	-13°	197°	55°

*$\vec{B}$ derived from Jensen and Cain [1962] coefficients

**Convention: if particle velocity vector $\vec{v} \parallel \vec{B}$, $\alpha \equiv 0°$

Acknowledgements

References

Anderson, K. A, Energetic electron fluxes in the tail of the
    geomagnetic field, J. Geophys. Res., 70, 4741-4763,
    1965.

Anderson, K. A., and N. F. Ness, Correlation of magnetic fields
    and energetic electrons on the IMP 1 satellite,
    J. Geophys. Res., 71, 3705-3727, 1966.

Cahill, L. J., Inflation of the magnetosphere near 8 earth
    radii in the dark hemisphere, J. Geophys. Res., 71,
    4505-4519, 1966.

Coon, James, Vela satellite measurements of particles in the
    solar wind and the distant geomagnetosphere, Radiation
    Trapped in the Earth's Magnetic Field, ed. by B. M.
    McCormac, D. Reidel, 231-255, 1966.

Davis, L. R., Low energy trapped protons and electrons,
    Proceedings of the Plasma Space Science Symposium,
    ed. by C. C. Chang and S. S. Huang, 214-226, 1965.

Frank, L. A., A survey of electrons E > 40 keV beyond 5 earth
    radii with Explorer XIV, J. Geophys. Res., 70, 1593-
    1626, 1965.

Frank, L. A., Explorer 12 observations of the temporal variations of low-energy electron intensities in the outer radiation zone during geomagnetic storms, J. Geophys. Res., 71, 4631-4639, 1966a.

Frank, L. A., Initial observations of low-energy electrons in the earth's magnetosphere with OGO 3, accepted for publication (September), J. Geophys. Res., 1966b.

Frank, L. A., Observations of magnetospheric boundary phenomena, Radiation Trapped in the Earth's Magnetic Field, ed. by B. M. McCormac, D. Reidel, 422-446, 1966c.

Freeman, J. W., The morphology of the electron distribution in the outer radiation zone and near the magnetospheric boundary as observed by Explorer XII, J. Geophys. Res., 69, 1691-1723, 1964.

Gringauz, K. I., V. G. Kurt, V. I. Moroz, and I. S. Shklovskii, Results of observations of charged particles observed out to R = 100,000 km, with the aid of charged-particle traps on Soviet space rockets, Astron. Zh., 37, 716-735 (1960; translation in: Soviet Astronomy-A.J., 4, 680-695, 1961).

Gringauz, K. I., V. V. Bezrukikh, L. S. Musatov, R. E. Rybchinsky, and S. M. Sheronova, Measurements made in the earth's magnetosphere by means of charged particle traps aboard the Mars I probe, Space Research, IV, 621-626, 1963.

Hoffman, R. A., and P. A. Bracken, Magnetic effects of the quiet time proton belt, J. Geophys. Res., 70, 3541-3556, 1965.

Jensen, D. C., and J. C. Cain, An interim geomagnetic field (abstract), J. Geophys. Res., 67, 3568-3569, 1962.

Nakada, M. P., J. W. Dungey, and W. N. Hess, On the origin of outer-belt protons, 1., J. Geophys. Res., 70, 3529-3532, 1965.

Ness, N. F., The earth's magnetic tail, J. Geophys. Res., 70, 2989-3003, 1965.

Ness, N. F., C. S. Scearce, and J. B. Seek, Initial results of the IMP-1 magnetic field experiment, J. Geophys. Res., 69, 3531-3569, 1964.

Parker, E. N., Particle effects in the geomagnetic field, Radiation Trapped in the Earth's Magnetic Field, ed. by B. M. McCormac, D. Reidel, 302-320, 1966.

Wolfe, J. H., R. W. Silva, and M. A. Myers, Observations of the
solar wind during the flight of IMP 1, J. Geophys. Res.,
71, 1319-1340, 1966.

Figure Captions

Figure 1.   The responses of two of the OGO 3 LEPEDEA 'B'

(LEPEDEA, Low Energy Proton and Electron Differential

Energy Analyzer) channels, electrons ($5.8 \leq E \leq 10$ keV)

and protons ($30 \leq E \leq 48$ keV), and of the thin-windowed

213B G.M. tube as functions of magnetic shell parameter

L for the outbound pass on 13 June 1966.

Figure 2.   Several useful position coordinates for OGO 3 on

13 June 1966 (outbound pass, Figure 1).

Figure 3.   Responses of three of the OGO 3 LEPEDEA 'B' channels,

protons ($450 \leq E \leq 720$ eV and $16 \leq E \leq 26$ keV) and

electrons ($1.5 \leq E \leq 2.7$ keV) as functions of L for the

outbound pass on 15 June 1966.

Figure 4.   Several useful position coordinates for OGO 3 on

15 June 1966 (outbound pass, Figure 3).

Figure 5.   Unidirectional intensities of protons ($330 \leq E \leq 530$ eV,

$450 \leq E \leq 720$ eV and $1.8 \leq E \leq 2.9$ keV) as functions of

L for the outbound OGO 3 traversal of the outer radiation

zone. Intensities are plotted as ●, upper limits as O.

Figure 6.   Continuation of Figure 5 for protons ($4.7 \leq E \leq 7.6$ keV

and $6.7 \leq E \leq 11$ keV).

Figure 7.   Continuation of Figure 5 for protons ($11 \leq E \leq 18$ keV,

$16 \leq E \leq 26$ keV and $30 \leq E \leq 48$ keV).

Figure 8.   Proton unidirectional intensities within six energy

bandpasses of LEPEDEA 'B' as functions of L for L $\sim$ 7.5

to 12.5 as observed during the outbound pass on 11 June

1966.

Figure 9.   Several useful position coordinates for OGO 3 on

11 June 1966 (outbound pass, Figure 8).

Figure 10.   Simultaneous observations of low-energy proton and

electron differential energy spectrums at L = 3.9,

07:04 U.T. on 15 June 1966.

Figure 11.   Comparison of OGO 3 observations of the proton

($1.8 \leq E \leq 48$ keV) differential energy spectrum on

15 June 1966 with Explorer 14 measurements of the proton

($E \geq 97$ keV) spectrum in late 1962 as reported by Davis

[1965] at L = 6.0, $\lambda_m = 24°$.   (E.P.A., equatorial pitch angle).

Omnidirectional intensities of protons ($1.8 \leq E \leq 48$ keV)

are 2 ($\pm$ 1) x 10^8 (cm^2-sec)$^{-1}$ at this position in the

outer radiation zone.

Figure 12. Simultaneous observations of proton and electron

spectrums at geocentric radial distance 10.5 R_E on

15 June 1966. If these spectrums are described by a

power law, $\frac{dJ}{dE} = kE^{-n}$, for $E \gtrsim 3$ keV, then $n \sim 1.8$

for the proton spectrum and $n \sim 3.8$ for the electron

spectrum. (See also Figure 3 for position relative to

charged particle distributions.)

Figure 13. An example of simultaneous observations of proton

and electron spectrums in the late evening sector of

the earth's magnetic tail at 15.9 R_E on 14 June 1966.
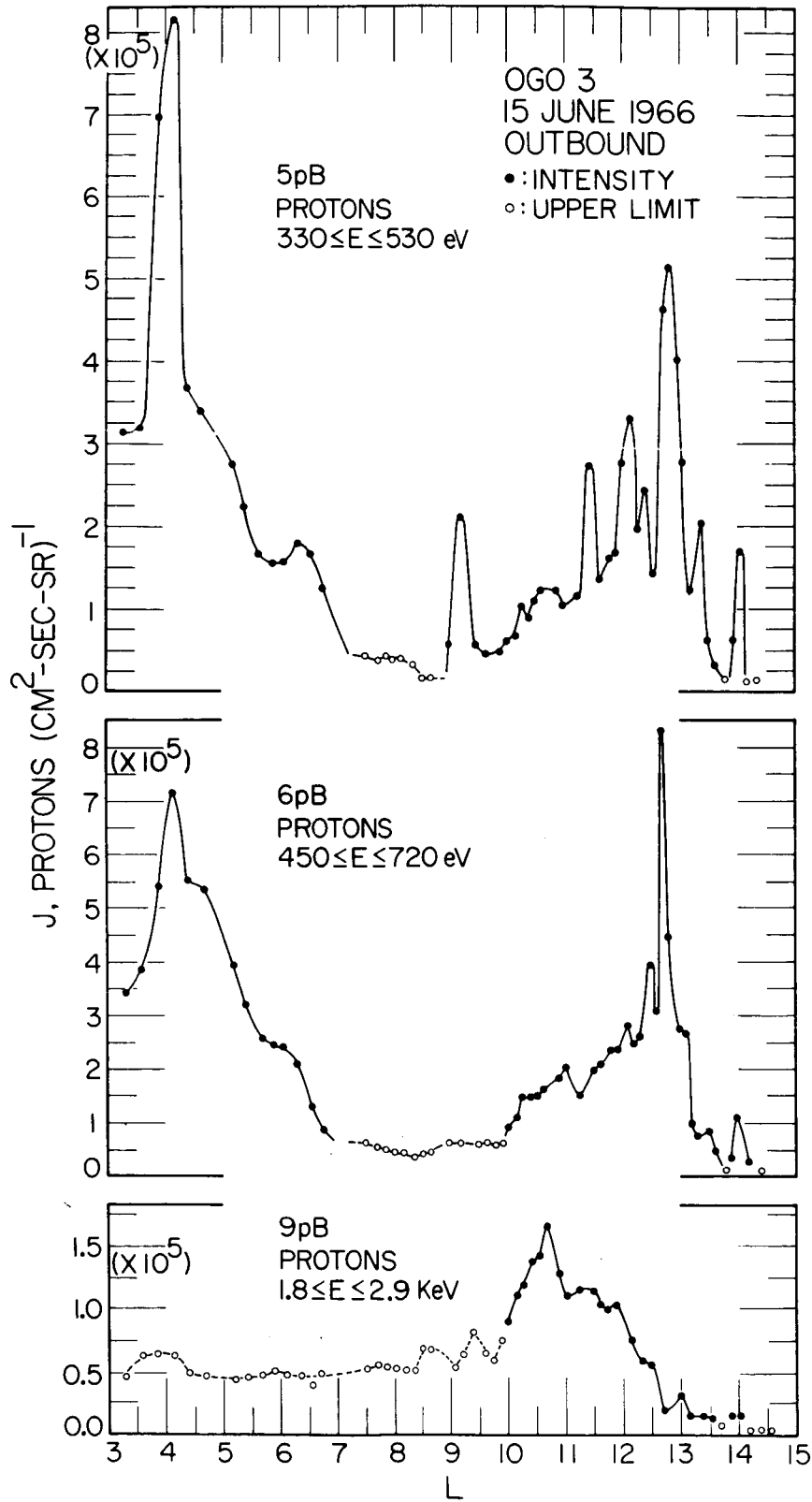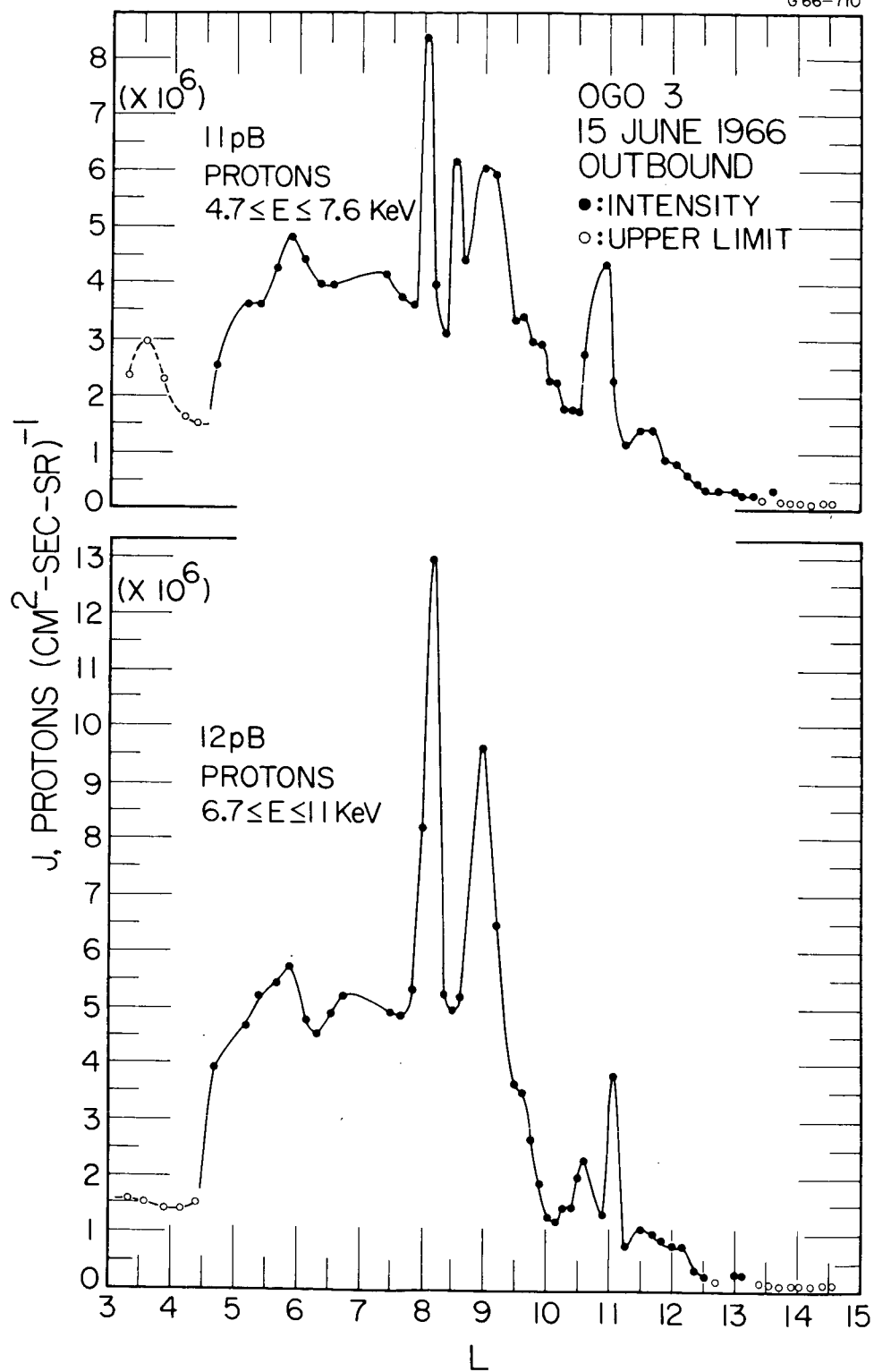
The sun-earth-probe (satellite) angle, θ_{SEP}, was 139°.
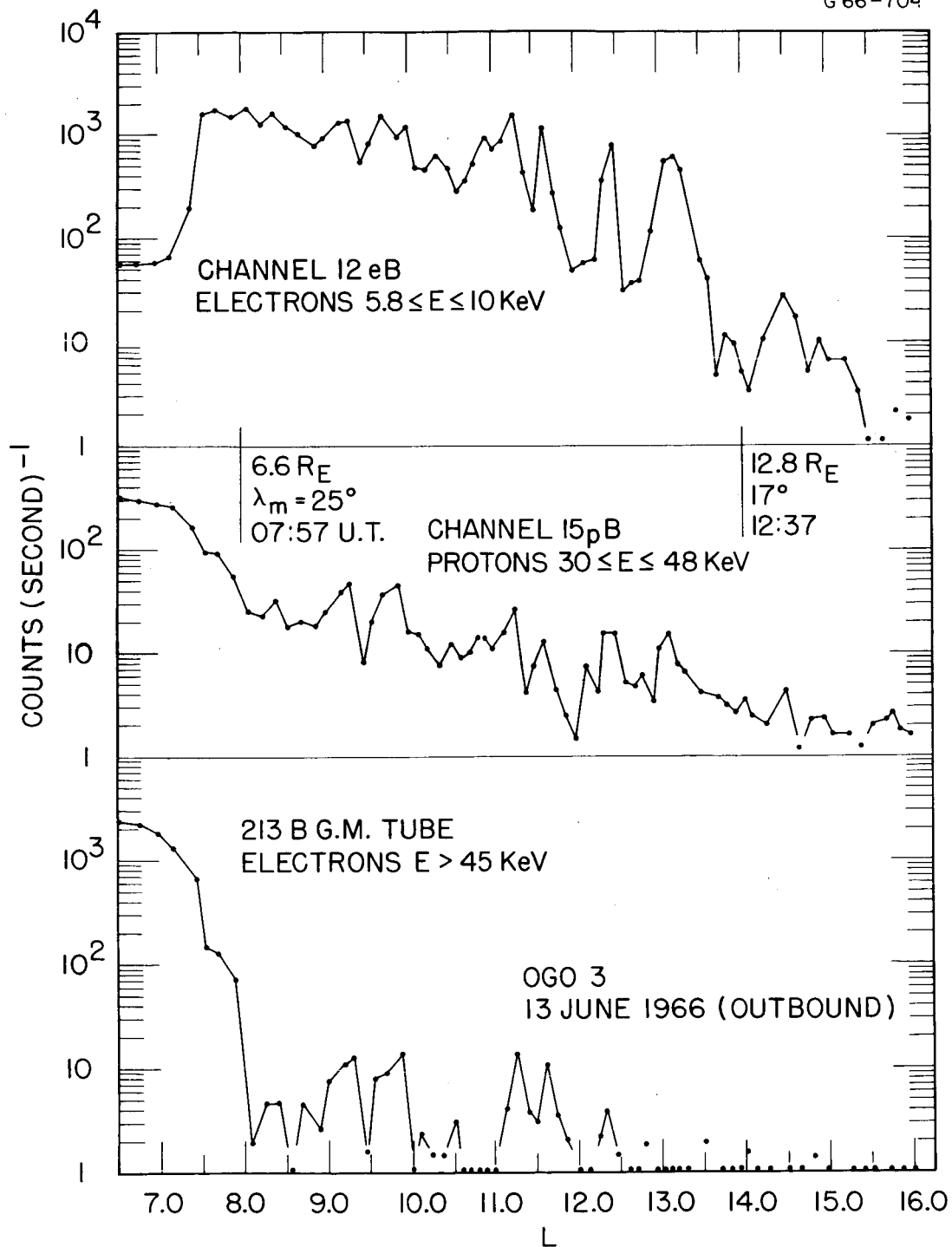
Figure 1
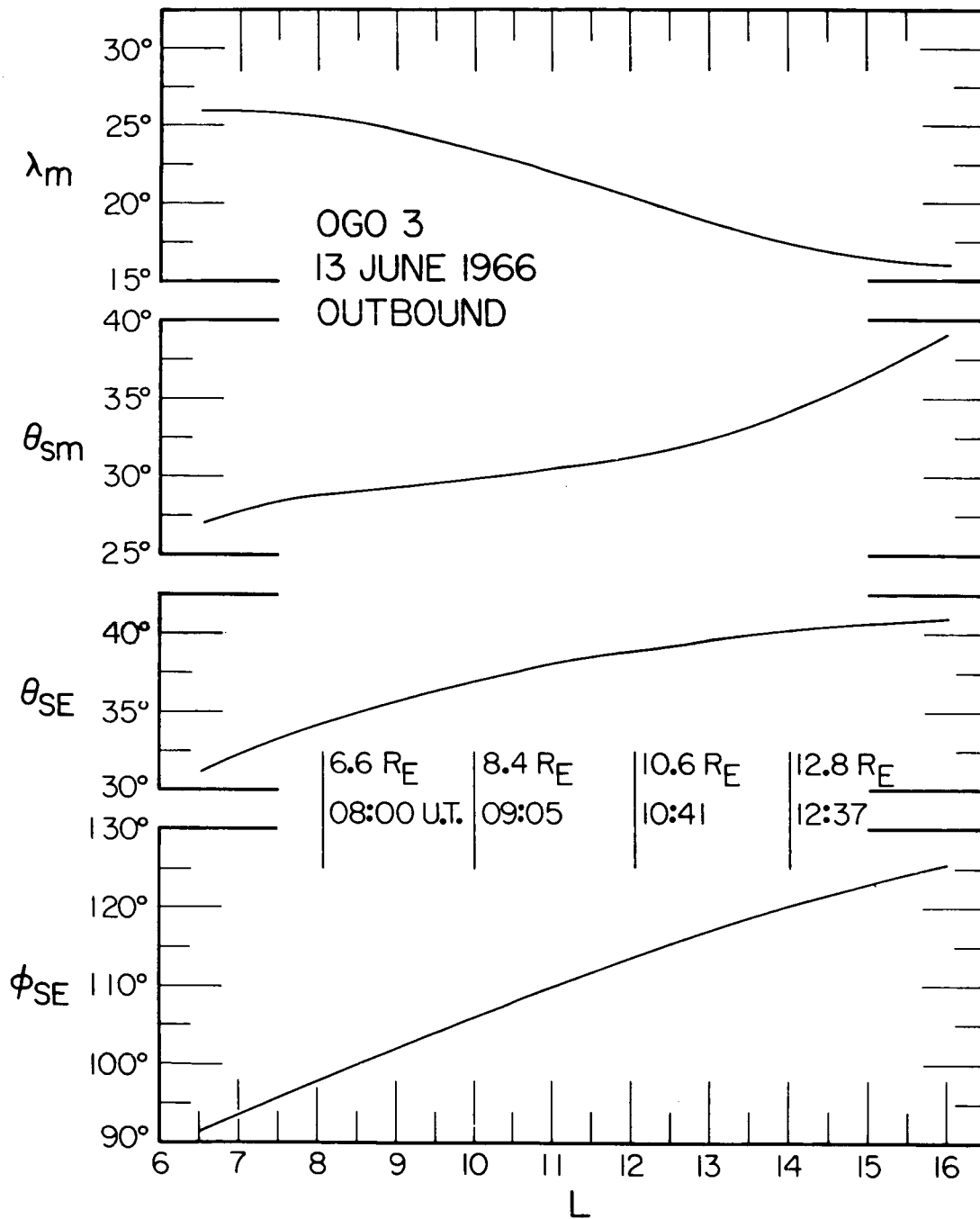
Figure 2
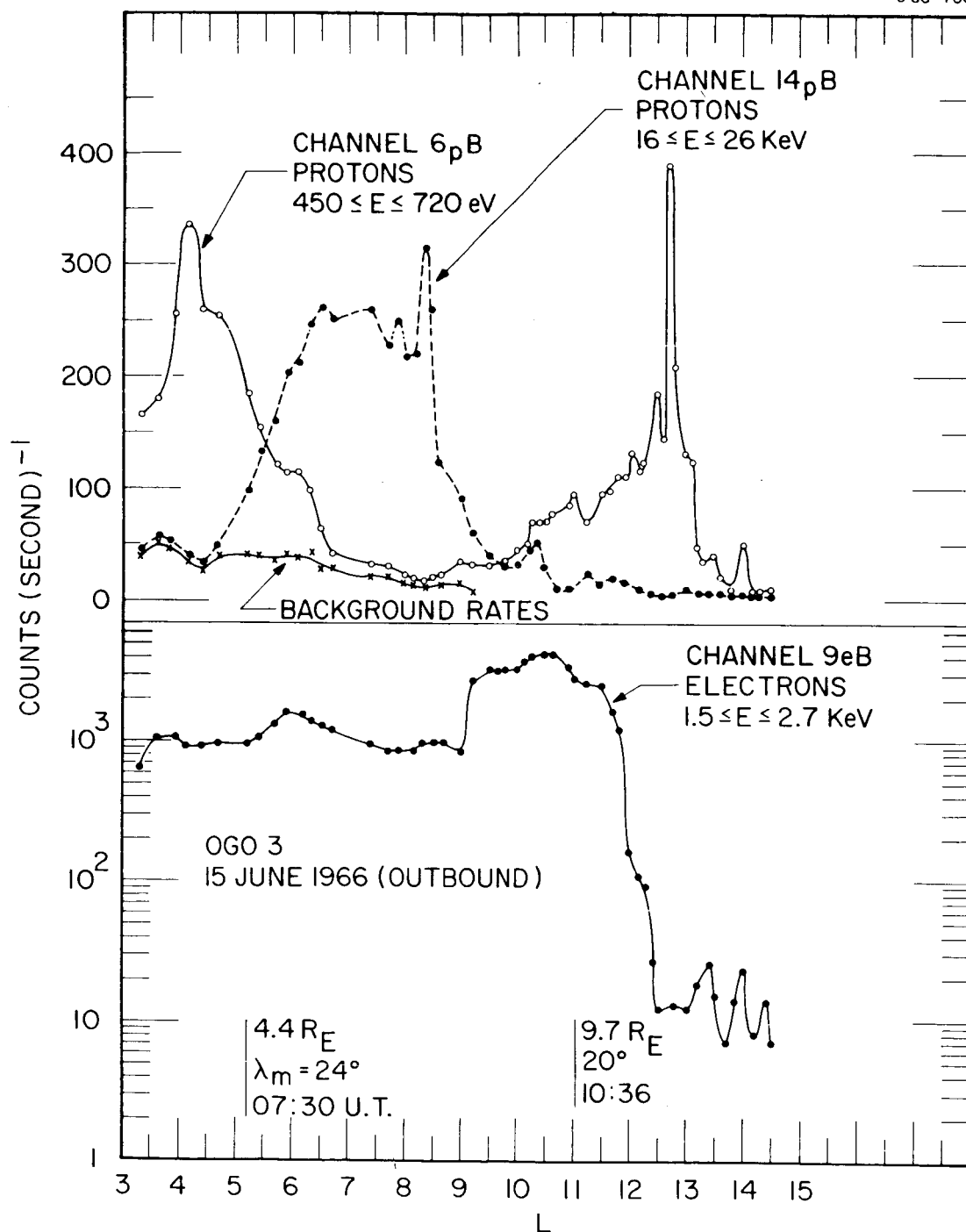
Figure 3
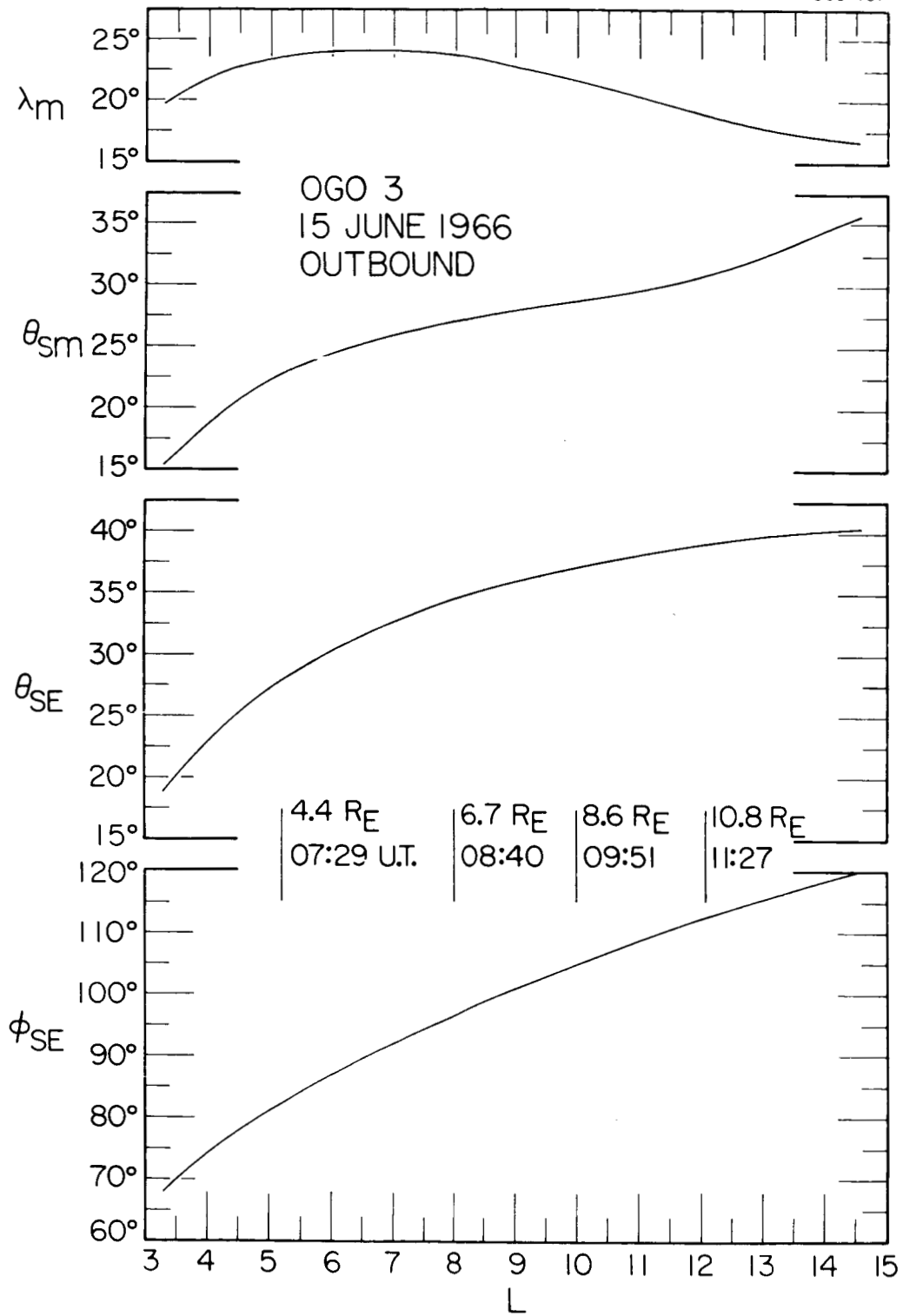
Figure 4

Figure 5

Figure 6

G 66-708

OGO 3
15 JUNE 1966
OUTBOUND
● : INTENSITY
○ : UPPER LIMIT

$13_p B$
PROTONS
$11 \leq E \leq 18$ KeV

$14_p B$
PROTONS
$16 \leq E \leq 26$ KeV

$15_p B$
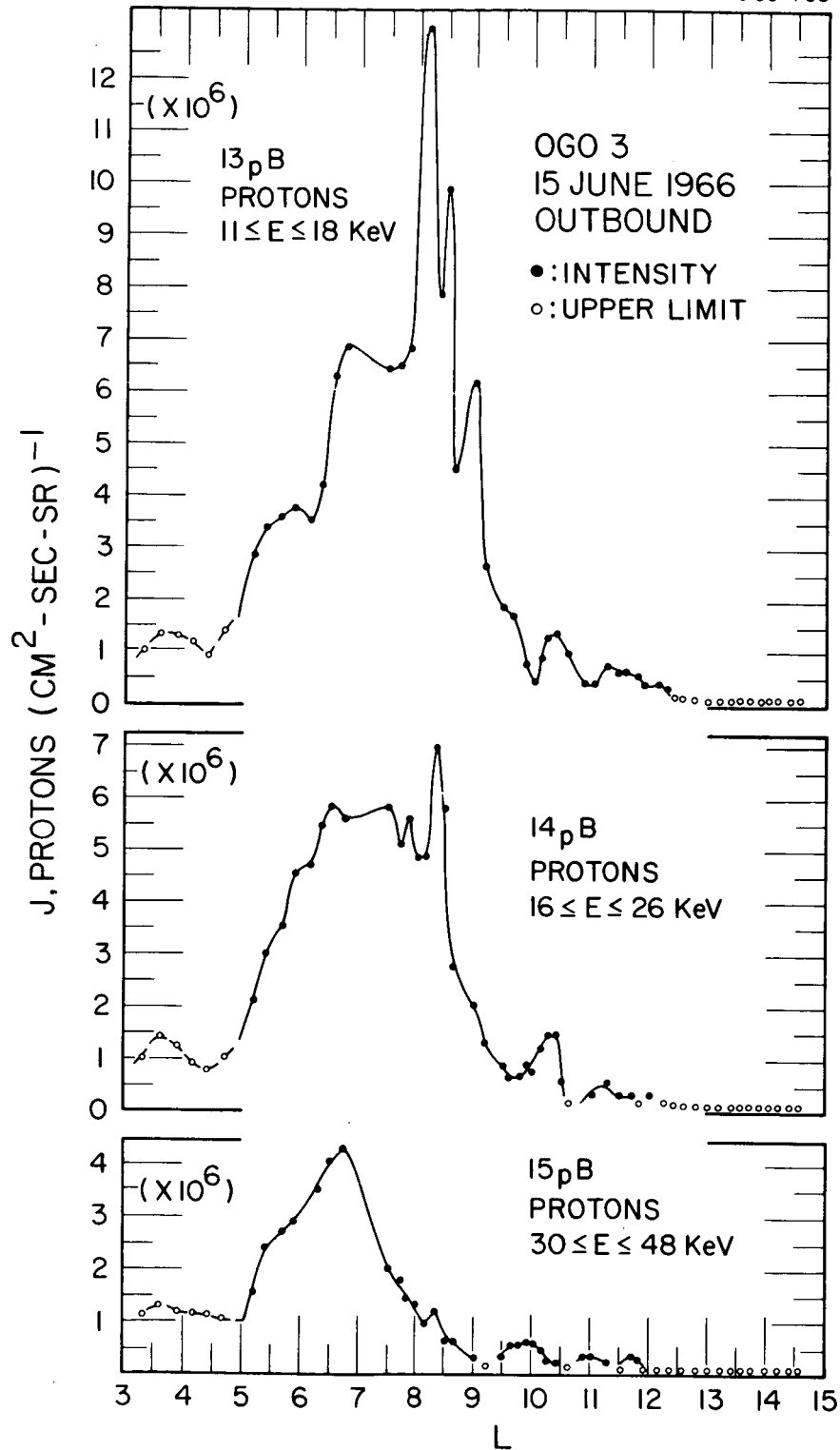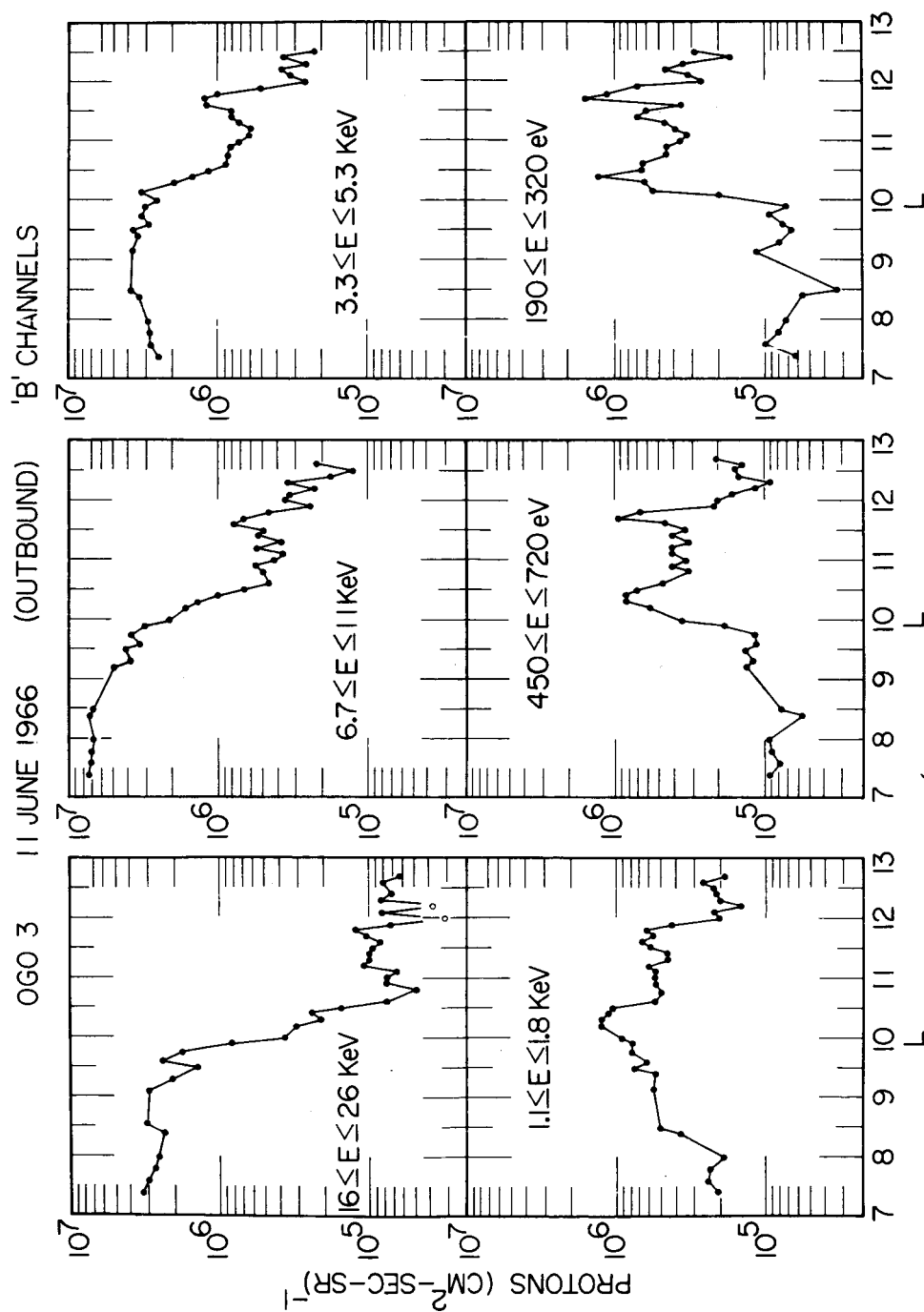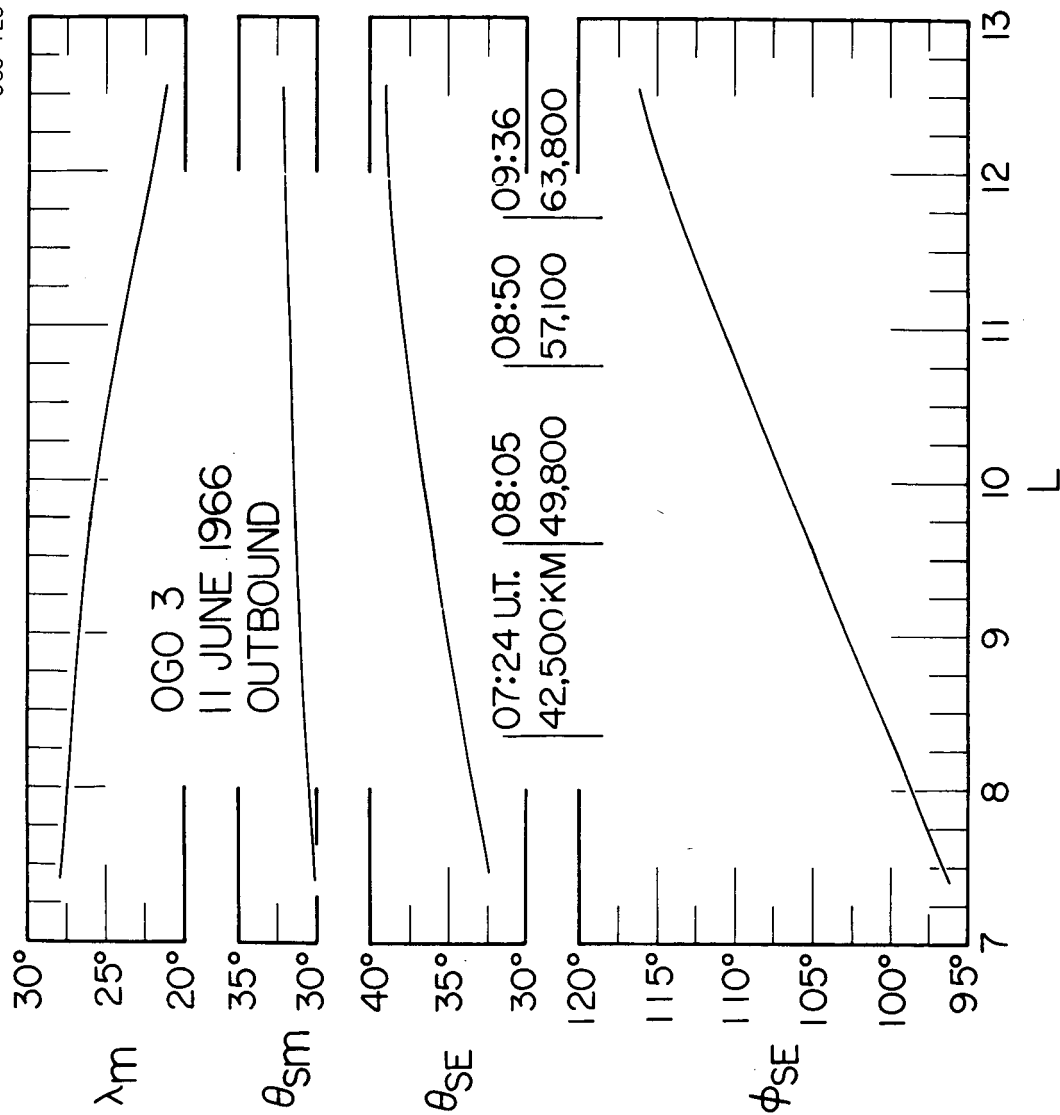PROTONS
$30 \leq E \leq 48$ KeV

J, PROTONS $(CM^2 - SEC - SR)^{-1}$

L

Figure 7

Figure 8

Figure 9
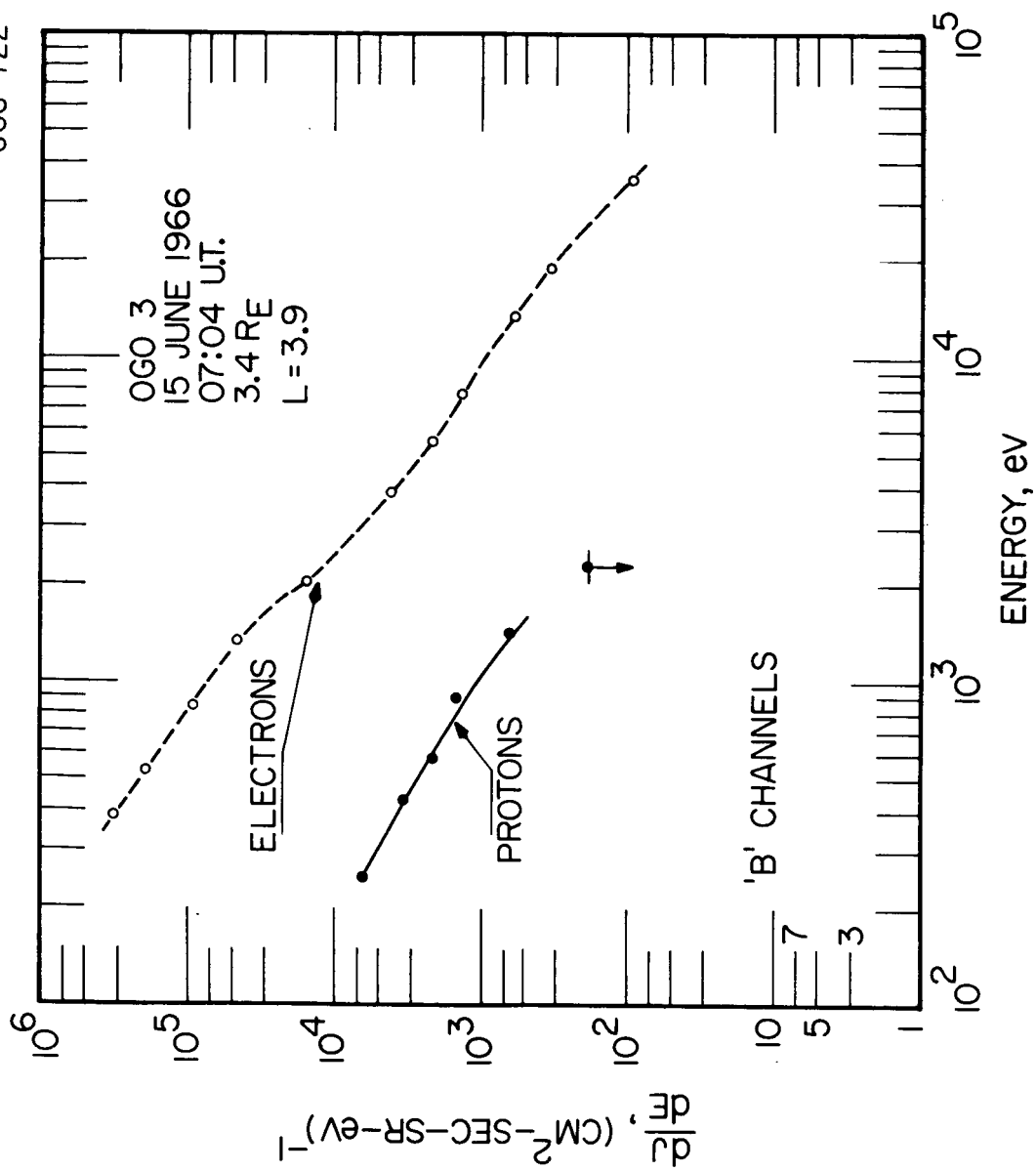
Figure 10

Figure 11

Figure 12

G66-725

OGO 3
14 JUNE 1966
19:14 U.T.
15.9 R_E
θ_{SEP} = 139°

ELECTRONS

PROTONS

'B' CHANNELS

7
3

$\frac{dJ}{dE}$, $(CM^2\text{-}SEC\text{-}SR\text{-}eV)^{-1}$

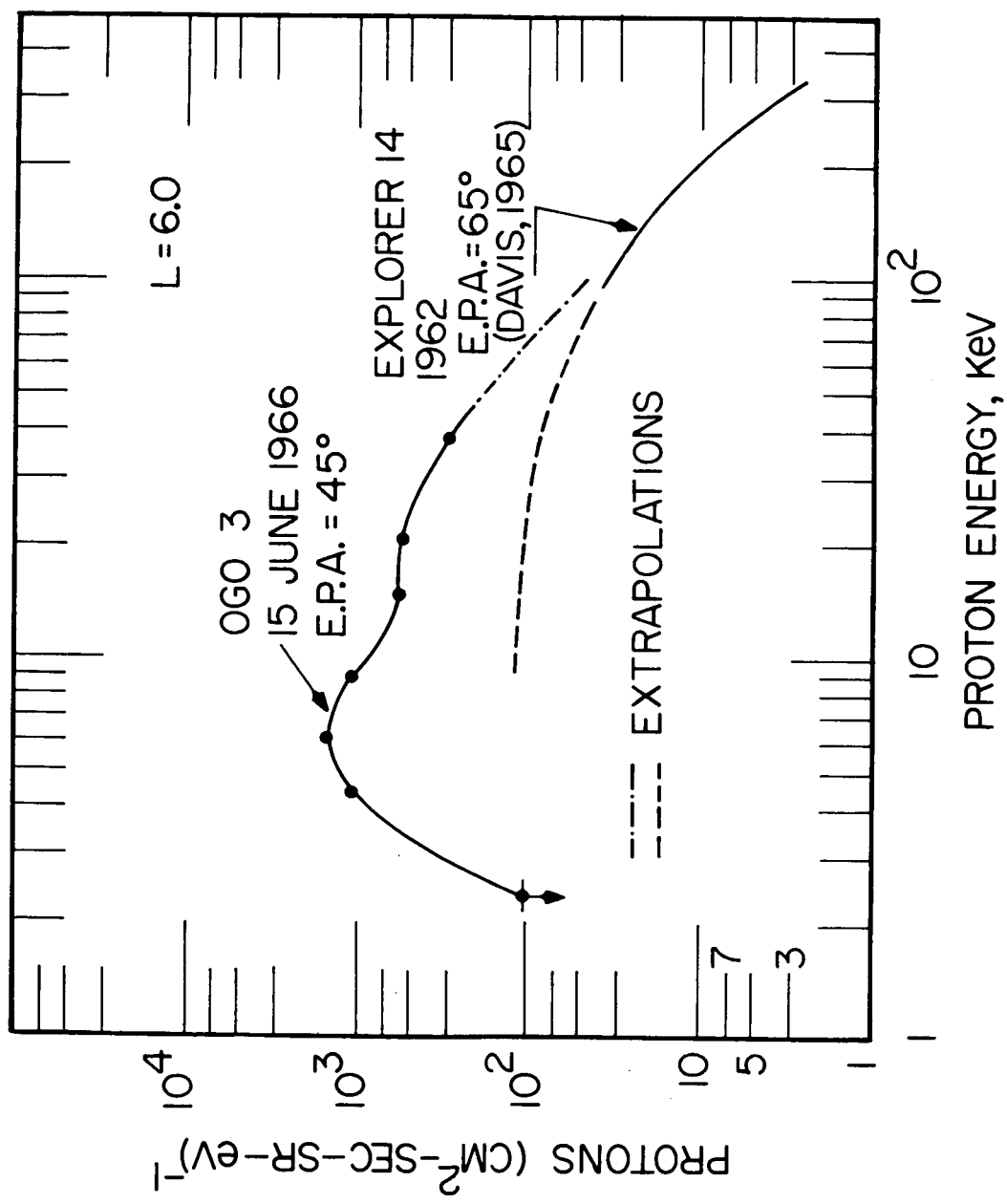ENERGY, eV
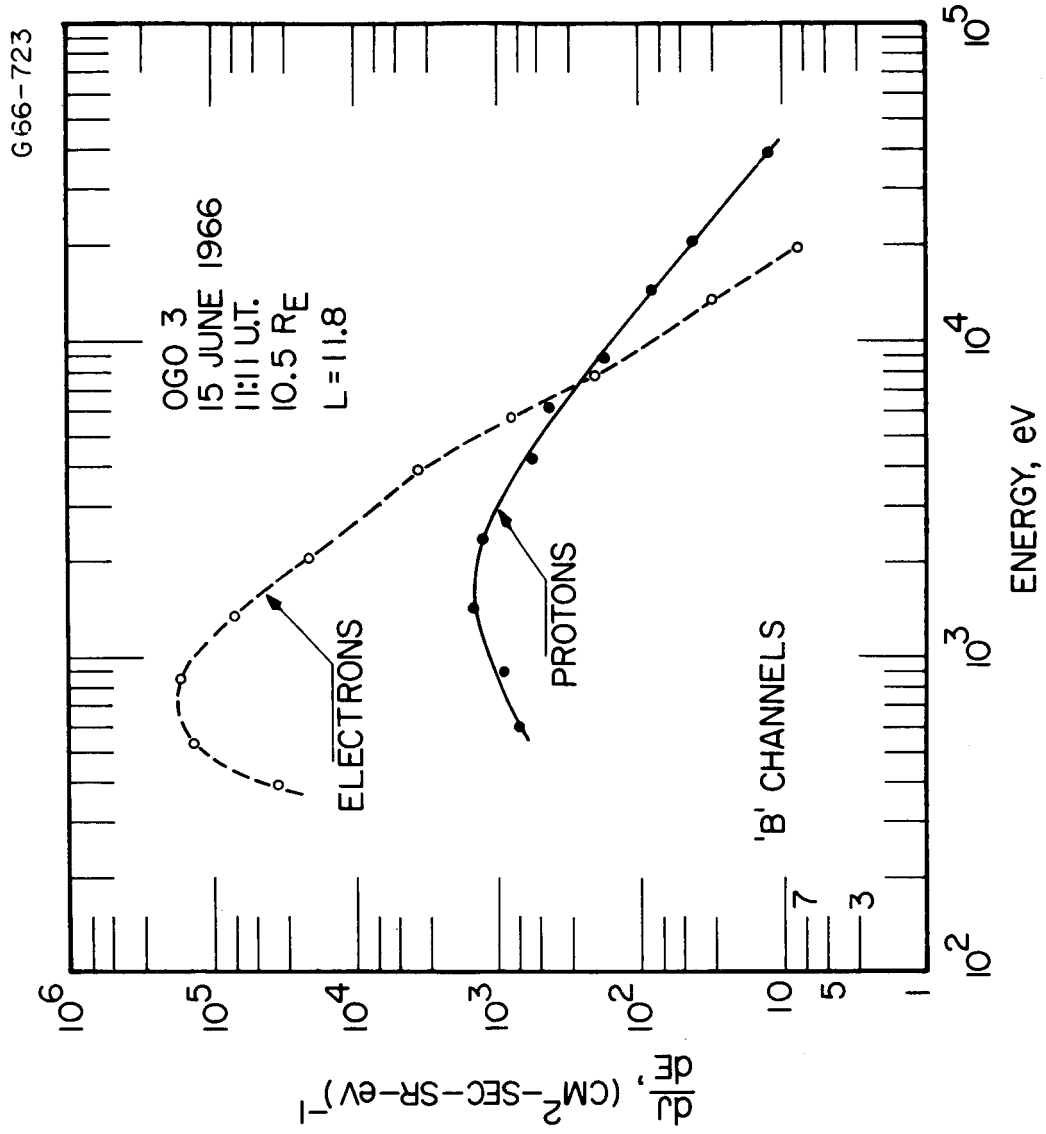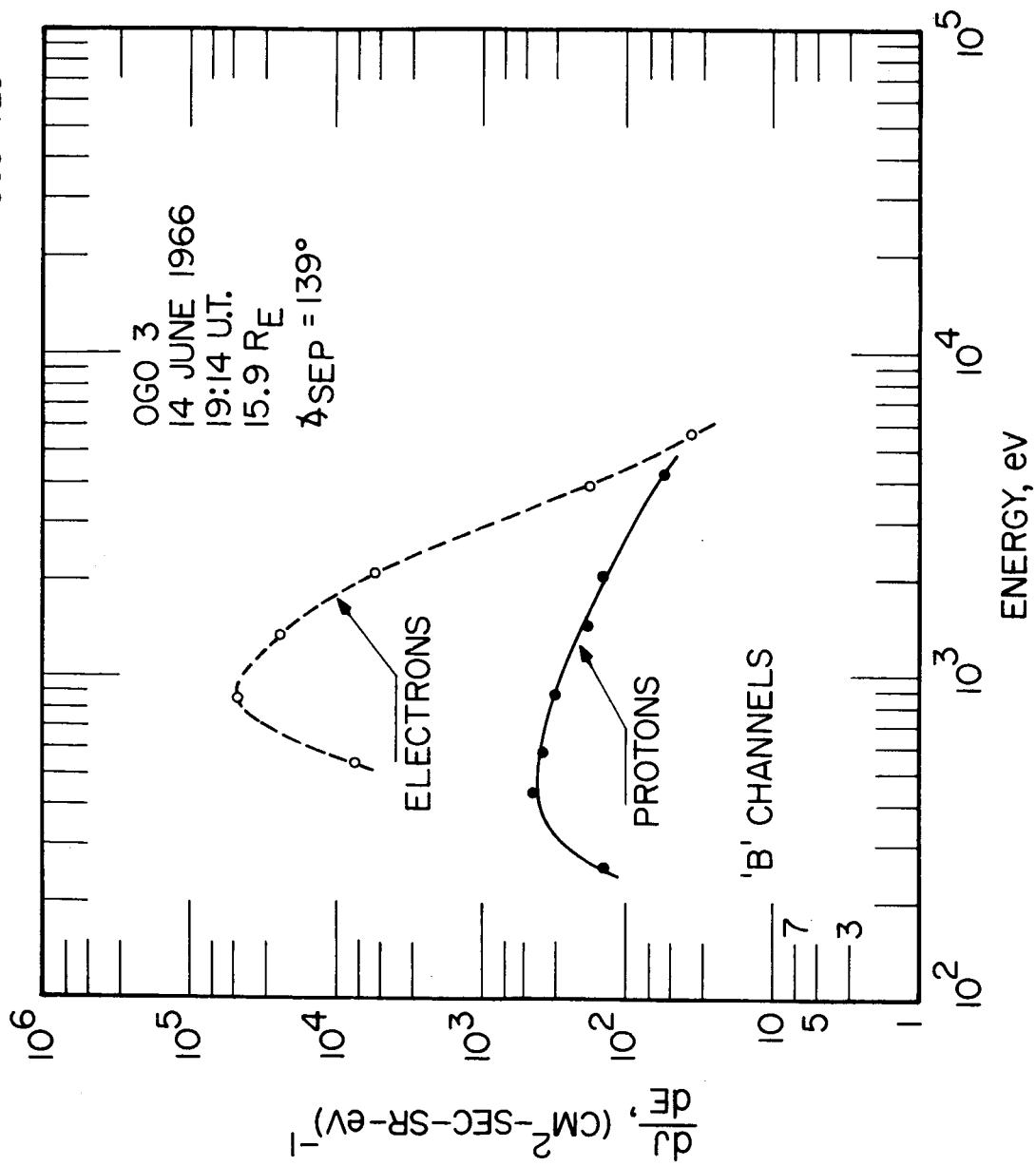
Figure 13

DOCUMENT CONTROL DATA - R&D

(Security classification of title, body of abstract and indexing annotation must be entered when the overall report is classified)

1. ORIGINATING ACTIVITY *(Corporate author)*	2a. REPORT SECURITY CLASSIFICATION
University of Iowa Department of physics and Astronomy	UNCLASSIFIED
	2b. GROUP

3. REPORT TITLE

Several Observations of Low-Energy Protons and Electrons in the Earth's Magnetosphere with OGO 3.

4. DESCRIPTIVE NOTES *(Type of report and inclusive dates)*

Progress   November 1966

5. AUTHOR(S) *(Last name, first name, initial)*

Frank, L. A.

6. REPORT DATE	7a. TOTAL NO. OF PAGES	7b. NO. OF REFS
November 1966	51	19

8a. CONTRACT OR GRANT NO.　Nonr-1509(06)	9a. ORIGINATOR'S REPORT NUMBER(S)
b. PROJECT NO.	U. of Iowa 66-48
c.	9b. OTHER REPORT NO(S) *(Any other numbers that may be assigned this report)*
d.	

10. AVAILABILITY/LIMITATION NOTICES

Distribution of this document is unlimited.

11. SUPPLEMENTARY NOTES　'	12. SPONSORING MILITARY ACTIVITY
	Office of Naval Research

13. ABSTRACT Simultaneous observations of proton (190 eV $\leq$ E $\leq$ 48 keV) and electron (170 eV $\leq$ E $\leq$ 46 keV) differential energy spectrums during segments of three outbound traversals of OGO 3 through the magnetosphere for the period 11-15 June 1966 on L-shells 3.3 to 16 are presented. Proton intensities at L = 4 on 15 June 1966 were 8 × 10^5 (cm^2-sec-sr)$^{-1}$ (330 $\leq$ E $\leq$ 530 eV), $\lesssim$ 1.5 × 10^6 (cm^2-sec-sr)$^{-1}$ (4.7 $\leq$ E $\leq$ 7.6 keV) and $\lesssim$ 10^6 (cm^2-sec-sr)$^{-1}$ (16 $\leq$ E $\leq$ 26 keV) and at L = 7.5 were $\leq$ 5 × 10^4 (cm^2-sec-sr)$^{-1}$ (330 $\leq$ E $\leq$ 530 eV), 4 ×10^6 (cm^2-sec-sr)$^{-1}$ (4.7 $\leq$ E $\leq$ 7.6 keV) and 6 × 10^6 (cm^2-sec-sr)$^{-1}$ (16 $\leq$ E $\leq$ 26 keV) with local pitch angles 78° ($\pm$ 4°) and at a geomagnetic latitude 23° ($\pm$ 1°). Peak intensities of protons (30 $\leq$ E $\leq$ 48 keV) were observed at L $\sim$ 7.0. A preliminary order-of-magnitude estimate of the total energy of trapped protons (190 eV $\leq$ E $\leq$ 48 keV) within the earth's magnetosphere is 5 × 10^{21} ergs and the estimated contribution from this low-energy proton distribution to the quiet-time terrestrial ring current field at the earth's surface is $\sim$ -10 γ. A transient, narrow peak of relatively high low-energy proton and electron intensities within the energy range $\sim$ 300 eV to

DD FORM 1473
1 JAN 64

14. KEY WORDS	LINK A		LINK B		LINK C	
	ROLE	WT	ROLE	WT	ROLE	WT
Radiation Zones						
Earth's Magnetic Tail						
Terrestrial Ring Currents						
Low-Energy Charged Particles (magnetosphere)						

INSTRUCTIONS

1. ORIGINATING ACTIVITY: Enter the name and address of the contractor, subcontractor, grantee, Department of Defense activity or other organization (*corporate author*) issuing the report.

2a. REPORT SECURITY CLASSIFICATION: Enter the overall security classification of the report. Indicate whether "Restricted Data" is included. Marking is to be in accordance with appropriate security regulations.

2b. GROUP: Automatic downgrading is specified in DoD Directive 5200.10 and Armed Forces Industrial Manual. Enter the group number. Also, when applicable, show that optional markings have been used for Group 3 and Group 4 as authorized.

3. REPORT TITLE: Enter the complete report title in all capital letters. Titles in all cases should be unclassified. If a meaningful title cannot be selected without classification, show title classification in all capitals in parenthesis immediately following the title.

4. DESCRIPTIVE NOTES: If appropriate, enter the type of report, e.g., interim, progress, summary, annual, or final. Give the inclusive dates when a specific reporting period is covered.

5. AUTHOR(S): Enter the name(s) of author(s) as shown on or in the report. Enter last name, first name, middle initial. If military, show rank and branch of service. The name of the principal author is an absolute minimum requirement.

6. REPORT DATE: Enter the date of the report as day, month, year; or month, year. If more than one date appears on the report, use date of publication.

7a. TOTAL NUMBER OF PAGES: The total page count should follow normal pagination procedures, i.e., enter the number of pages containing information.

7b. NUMBER OF REFERENCES: Enter the total number of references cited in the report.

8a. CONTRACT OR GRANT NUMBER: If appropriate, enter the applicable number of the contract or grant under which the report was written.

8b, 8c, & 8d. PROJECT NUMBER: Enter the appropriate military department identification, such as project number, subproject number, system numbers, task number, etc.

9a. ORIGINATOR'S REPORT NUMBER(S): Enter the official report number by which the document will be identified and controlled by the originating activity. This number must be unique to this report.

9b. OTHER REPORT NUMBER(S): If the report has been assigned any other report numbers (*either by the originator or by the sponsor*), also enter this number(s).

10. AVAILABILITY/LIMITATION NOTICES: Enter any limitations on further dissemination of the report, other than those imposed by security classification, using standard statements such as:

(1) "Distribution of this document is unlimited."

(2) "Foreign announcement and dissemination of this report by DDC is not authorized."

(3) "U. S. Government agencies may obtain copies of this report directly from DDC. Other qualified DDC users shall request through
_____ ."

(4) "U. S. military agencies may obtain copies of this report directly from DDC. Other qualified users shall request through
_____ ."

(5) "All distribution of this report is controlled. Qualified DDC users shall request through
_____ ."

If the report has been furnished to the Office of Technical Services, Department of Commerce, for sale to the public, indicate this fact and enter the price, if known.

11. SUPPLEMENTARY NOTES: Use for additional explanatory notes.

12. SPONSORING MILITARY ACTIVITY: Enter the name of the departmental project office or laboratory sponsoring (*paying for*) the research and development. Include address.

13. ABSTRACT: Enter an abstract giving a brief and factual summary of the document indicative of the report, even though it may also appear elsewhere in the body of the technical report. If additional space is required, a continuation sheet shall be attached.

It is highly desirable that the abstract of classified reports be unclassified. Each paragraph of the abstract shall end with an indication of the military security classification of the information in the paragraph, represented as (*TS*), (*S*), (*C*), or (*U*).

There is no limitation on the length of the abstract. However, the suggested length is from 150 to 225 words.

14. KEY WORDS: Key words are technically meaningful terms or short phrases that characterize a report and may be used as index entries for cataloging the report. Key words must be selected so that no security classification is required. Identifiers, such as equipment model designation, trade name, military project code name, geographic location, may be used as key words but will be followed by an indication of technical context. The assignment of links, roles, and weights is optional.

DD FORM 1 JAN 64 1473 (BACK)

Continuation of Item 13, ABSTRACT:

2 keV at L $\sim$ 4 with width $\Delta L \sim 1$ is also observed. Typical characteristics
of proton and electron intensity 'spikes' at peak intensities in the
late evening sector of the earth's magnetic tail are (a) approximately
equal proton (190 eV $\le$ E $\le$ 48 keV) and electron (170 eV $\le$ E $\le$ 46 keV)
energy densities, $\sim 10^{-9}$ erg(cm)$^{-3}$ each, (b) approximately equal
proton and electron densities over the above energy range, ~ 1 (cm)$^{-3}$
each, and (c) largely dissimilar differential energy spectrums,
proton spectrums with intensity peaks noncoincident in energy with
those of the electron intensity peaks and significantly broader
(harder) in the high-energy tail (E $\gtrsim$ 3 keV) than the relatively
steep (soft) electron spectrums in this energy range.